CHEMISTRY
A EUROPEAN JOURNAL

DOI: 10.1002/chem.200500976

Guest Encapsulation and Self-Assembly of a Cavitand-Based Coordination Capsule

Takeharu Haino,* Mutsumi Kobayashi, and Yoshimasa Fukazawa*[a]

Abstract: The synthesis and spectroscopic characterization of a cavitand-based coordination capsule **1·4BF$_4$** of nanometer dimensions is described. Encapsulation studies of large aromatic guests as well as aliphatic guests were performed by using ^{1}H NMR spectroscopy in [D$_1$]chloroform. In addition to the computational analysis of the shape and geometry of the capsule, an experimental approach to estimate the interior size of the cavity is discussed. The cavity provides a highly rigid binding space in which molecules with lengths of approximately 14 Å can be selectively accommodated. The rigid cavity distinguished slight structural differences in the flexible alkyl-chain guests as well as the rigid aromatic guests. The detailed thermodynamic studies revealed that not only CH–π interactions between the methyl groups on the guest termini and the aromatic cavity walls, but also desolvation of the inner cavity play a key role in the guest encapsulation. The cavity preferentially selected the hydrogen-bonded heterodimers of a mixture of two or three carboxylic acids **18**–**20**. The chiral capsule encapsulated a chiral guest to show diastereoselection.

Keywords: cavitands · metal coordination · molecular recognition · self-assembly · supramolecular chemistry

Introduction

Cavitand-based molecular containers provide enforced cavities surrounded by aromatic hemispheres, showing unique guest-encapsulation properties.[1] Cram and co-workers have developed molecular containers consisting of two cavitands with covalent linkages, so-called "carcerands" and "hemicarcerands", which provide the confined inner cavities.[2] A wide variety of guests of different size, shape, charge, and stability were entrapped within their interiors. The recent strategy to construct confined inner cavities surrounded by hemispheres is based on self-assembly by hydrogen-bonding interactions. Resorcinarene-based self-assembling cylindrical dimers and hexameric assemblies have been developed.[3,4] Their nanometric cavities are large enough to bind sizable guests or even more than one guest molecule. Particularly impressive features of the cavities are their ability to stabilize reactive intermediates and unusual molecular species within the interior, to control and change the reaction rates and regiochemistry, and to amplify and catalyze reactions.

Metal-coordination-driven self-assembly has become another tool for creating a variety of multicomponent self-assemblies because a large number of combinations of coordination motifs and ligands are available. Thus, metal-directed self-assembly is intensely developed as a promising approach to generate supramolecular architectures possessing nanometric cavities.[5] Such structures may find use in many potential applications: as reaction vessels, catalysts, drug containers, molecular switches, memory storage devices, and others. In particular, cavitand-based coordination capsules and cages have received a great deal of attention due to their unique guest-binding properties, arising from their discrete cavities. Introduction of four ligation sites (pyridyl, nitrile, dithiocarbamate, and others) on the upper rim of the cavitands provides the tetradentate ligands, which can assemble to form a capsule or a cage by means of metal ligation.[6] We previously reported the synthesis and the binding properties of a new self-assembling capsule in which two octadentate cavitands possessing four bipyridyl groups complex with four silver cations in a tetrahedral fashion.[7] In this paper, we describe the experimental details of the synthesis and characterization of a nanosized self-assembling capsule **1·4BF$_4$**, and introduce probes that reveal the behavior of sizeable organic guests inside the cavity—their dimen-

[a] Prof. Dr. T. Haino, M. Kobayashi, Prof. Dr. Y. Fukazawa
Department of Chemistry, Graduate School of Science
Hiroshima University
1-3-1 Kagamiyama, Higashi-Hiroshima 739-8526 (Japan)
Fax: (+81) 82-424-0724
E-mail: haino@sci.hiroshima-u.ac.jp
fukazawa@sci.hiroshima-u.ac.jp

sions and stability. Thereafter we discuss the thermodynamic study of guest encapsulation by the capsule. The pairwise interactions of small guest dimers and the diastereoselective binding of a chiral guest within the capsule are presented.

Results and Discussion

Design, synthesis, and characterization of self-assembled capsule 1: A methylene-bridged cavitand has a small cavity in which small guests can be accommodated.[1c] Octadentate cavitand **2** has a large cavity, expanded by the introduction of four aromatic spacers on its upper rim. Self-assembly of two of the expanded cavities by silver coordination in a tetrahedral fashion offers the easy construction of an extremely large guest binding space (Scheme 1). According to molecular modelling by MacroModel V.6.5 with the amber* force field,[8] the calculated structure of **1** has a large cavity, with the volume estimated to be $\approx 580\ Å^3$ by the Grasp program.[9] This large cavity can show highly selective binding of small guest pairs as well as large guests. Cavitand-based chiral assembly has been limited so far. Chiral, assembled capsule **1** exhibits D_4 symmetry. Encapsulation of a chiral guest should give rise to diastereomeric complexes.

The synthesis of cavitand **2** was performed according to Scheme 2. The phenyl spacer was attached to bipyridine **3**[10] by Suzuki coupling with diboronate **4**,[11] which afforded bipyridine **5** in a good yield. The synthesis of the new cavitand began with tetrabromocavitand **6** prepared as described earlier by Reinhoudt.[12] Cavitand **6** was treated with *n*BuLi and subsequent addition of iodine to give tetraiodocavitand **7**. A Suzuki coupling reaction[13] of **5** and **7** proceeded smoothly to give the desired octadentate cavitand **2**.

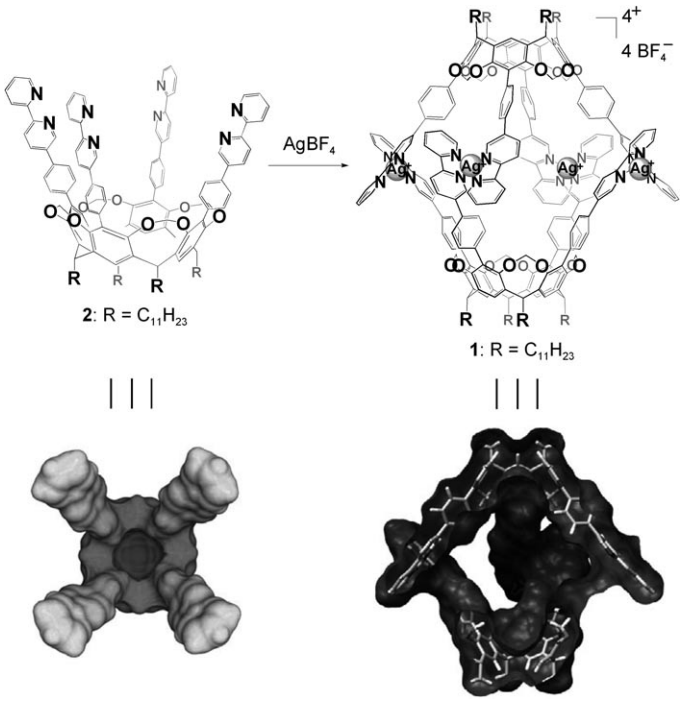

Scheme 1. Self-assembled capsule **1·4BF$_4$** and cavitand **2**. In the energy-minimized structures, the long alkyl chains are omitted for viewing clarity. Van der Waals surfaces are shown in each structure. Left: Top view of the cavitand. Right: Side view of the capsule. Some atoms have been removed to show the inner surface of the cavity.

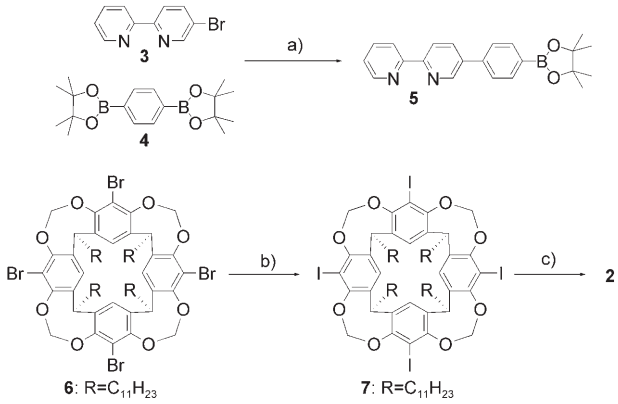

Scheme 2. Reagents and conditions: a) $[Pd(PPh_3)_4]$, Na_2CO_3, dioxane, H_2O, 49%; b) *n*BuLi, I_2, THF, 79%; c) $[PdCl_2(PPh_3)_2]$, Ph_3As, Cs_2CO_3, **5**, dioxane, 80%.

Capsule **1·4BF$_4$** was formed as a colorless solid by the addition of two equivalents of silver tetrafluoroborate to a solution of **2** in nitromethane. The elementary composition of **1·4BF$_4$** was confirmed by using combustion analysis. Because the versatility of electrospray ionization (ESI) mass spectrometry in determining the molecular weight and the isotopic distribution pattern of highly charged systems is well established, the ESI mass measurement of **1·4BF$_4$** was carried out (Figure 1). The mass spectrum shows several characteristic peaks, which were assigned to the dimeric structure of **1**. The four observed peaks (av $m/z = 4840$ (calcd 4841) $[\mathbf{1{\cdot}3BF_4}]^+$; av $m/z = 2378$ (calcd 2377) $[\mathbf{1{\cdot}2BF_4}]^{2+}$; av $m/z = 1556$ (calcd 1556) $[\mathbf{1{\cdot}BF_4}]^{3+}$; av $m/z = 1145$ (calcd 1145) $[\mathbf{1}]^{4+}$) belonged to species resulting from a consecutive loss of four tetrafluoroborate counterions from the +1 charged state to the +4 charged state. The experimental isotopic pattern of $[\mathbf{1{\cdot}BF_4}]^{3+}$ matched the calculated pattern very well. These results excluded the formation of tri- and tetrameric assemblies.

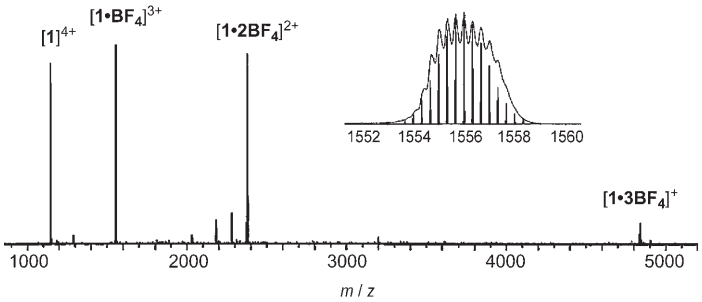

Figure 1. ESI MASS spectra of complex **1·4BF$_4$**. The inset shows the calculated (straight line) and the experimental isotopic pattern (curve) of $[\mathbf{1{\cdot}BF_4}]^{3+}$.

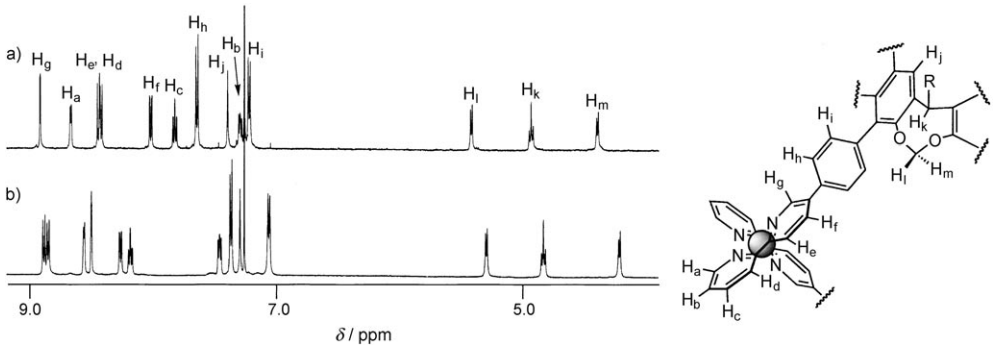

Figure 2. ^{1}H NMR spectra in [D_1]chloroform of a) **2** and b) **1·4BF$_4$**.

The ^{1}H NMR spectrum of the capsule gives detailed structural information (Figure 2). Self-assembly of two octadentate cavitands **2** with four silver cations might be expected to form many diastereomeric forms of the capsule; however, the ^{1}H NMR spectrum in $CDCl_3$ showed the selective formation of the D_4 symmetric form in which the eight bipyridyl groups are magnetically equivalent. Pyridyl protons H_a and H_g showed upfield shifts whereas downfield shifts were observed for H_b to H_f as a consequence of the Ag–N bond formation. In general, metal complexation to pyridine causes downfield shifts of the pyridyl protons. The irregular upfield shifts of protons H_a and H_g rationalizes the idea that a silver cation complexes to two bipyridine groups in a tetrahedral fashion; protons H_a and H_g stay in the shielding region of the other bipyridyl group and experience their shielding effect. Although the precise reason for the selective formation of the D_4 form remains to be determined, molecular modelling of **1·4BF$_4$** suggests that the D_4 symmetric form is more stable than the others.

The diffusion coefficient of a molecule depends on its size and shape. The Stoke–Einstein equation ($D = kT/6\pi\eta r$) shows that the diffusion coefficient (D) is inversely proportional to the hydrodynamic radius (r). Hence, by determining the ratio of the diffusion coefficients for two different molecules, the ratio of their radii is provided.[14] Diffusion NMR spectroscopy is an emerging technique in supramolecular chemistry. In recent years, this technique has been used to investigate issues of structure and mechanism in molecular assembly.[15,16] A number of theoretical studies have predicted that a dimer should have a diffusion coefficient (D) that is 72–75% of its corresponding monomer's value.[17]

To gain further evidence of the capsule formation in solution, we set out to determine diffusion coefficients for **1·4BF$_4$** and **2** by pulsed field gradient NMR using a bipolar pulse pairs stimulated echo (BPPSTE) pulse sequence. The influence of increasing magnetic field gradient strength (g) on the intensity of the terminal methyl proton signal of the alkyl chains for both **1·4BF$_4$** and **2** was monitored. The signal intensities of the protons for both molecules decayed as a function of the gradient strengths. The given data were fitted using the Stejskal–Tanner equation ($-\ln(I/I_0) = \gamma^2 g^2 \delta^2 (\Delta - \delta/3) D$, Figure 3) to give the diffusion coefficients ($3.66 \pm 0.05 \times 10^{-10}$ and $4.79 \pm 0.04 \times 10^{-10}$ m^{2}s^{-1} for **1·4BF$_4$** and **2**, respectively).[17] The resulting ratio $D_{dim}/D_{mono} = 0.76$ is in reasonable agreement with the theoretical ratio of 0.72–0.75 expected for a dimer and confirms the dimeric nature of the complex **1·4BF$_4$**.[18]

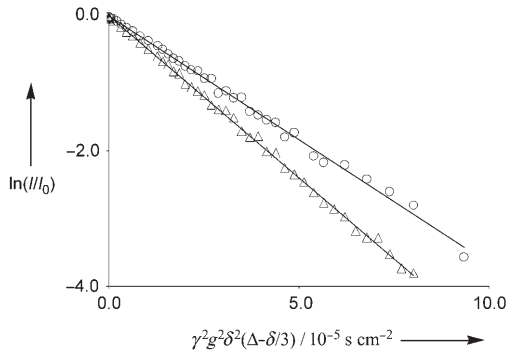

Figure 3. Stejskal–Tanner plot of **1·4BF$_4$** (○) and **2** (△) at 297 K in [D_1]chloroform.

Complex **1·4BF$_4$** is very stable in [D_1]chloroform. However, the kinetic stability of the complex in organic solution was not assessed. When a solution of **1·4BF$_4$** in [D_1]chloroform was added to that of **2**, their sharp signals appeared independently; this observation supports the existence of sizable energetic barriers between free and complexed states. To gain an insight into the dynamic behavior between the complexed and the free states, 2D EXSY spectra of the mixture was measured (Figure 4).[19] Exchange cross peaks were observed in the spectrum, revealing that dynamic exchange between them still exists, but that the rate is slower than the NMR timescale. In common Ag–bipyridine complexes, the energy barrier for the exchange between the free and the complexed states is small.[20] This high kinetic stability of capsule **1·4BF$_4$** would be a result of the cooperative complexation of the bipyridine units.

Encapsulation of guests by capsule 1·4BF$_4$: In molecular recognition the dimension and shape of an internal cavity of cavitands, carcerands, and capsules can usually be estimated by using molecular modelling, or more precisely, by using X-ray crystallography. Molecular modelling of the capsule based on MacroModel V.6.5 presented the extremely large dimension of its cavity: the distance from the bottom of the

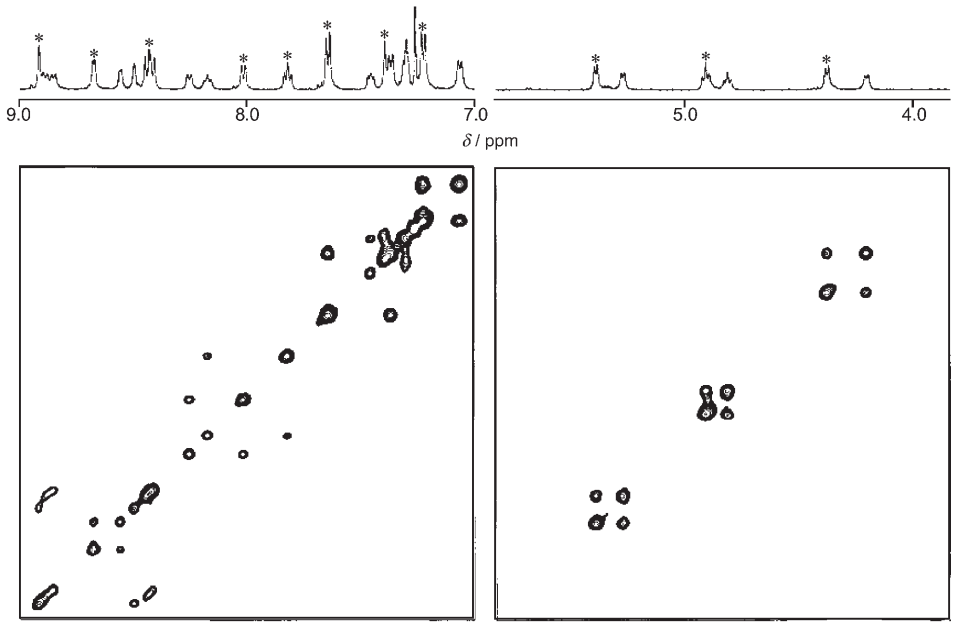

Figure 4. 2D EXSY spectrum of a mixture of **1·4BF$_4$** (0.40 mmol L^{-1}) and **2** (1.00 mmol L^{-1}). The signals of **2** are marked with *.

one cavitand to the other is about 16 Å, and the volume of the cavity is calculated to be ≈580 Å^3; however, cavitand **2** itself has a narrow cavity at the bottom end, complementary to only a methyl group. Accordingly, the selected guests have a methyl group on either one or both ends of their structure. The binding properties for guests **8**–**14** to capsule

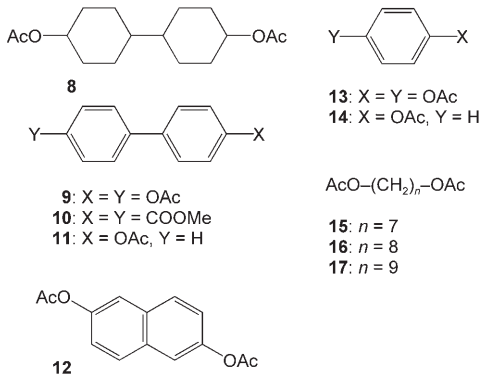

1·4BF$_4$ were assessed by using ^{1}H NMR spectroscopy. The reasonably rigid guests **8**–**10**, possessing lengths of 14.1–14.6 Å, were shown to be excellent guests for capsule **1·4BF$_4$**. They are also complementary in shape and functionality and long enough to occupy a sizable part of the internal cavity. In the resulting complexes, the signals of the bound and unbound guests did not overlap at room temperature, indicating that a sizable kinetic barrier exists between the exchange process of the guests in and out of the capsule at room temperature (Figure 5).

The large upfield shifts of the terminal methyl groups of guests **8**–**10** ($\Delta\delta = 3.7$ ppm) place them near the ends of capsule **1·4BF$_4$**. Intense intermolecular nuclear Overhauser effect (NOE) contacts were observed between the cavitand protons (H_j, H_l, and H_m shown in Figure 2) of **1·4BF$_4$** and the methyl groups of encapsulated **9**, thus indicating that its methyl groups are positioned deep inside the cavitand termini of the capsule (Figure 6). The calculated structures of the capsule with **8**–**10** help to explain the observed upfield shifts of the terminal methyl groups and the NOE contacts.

In contrast, shorter aromatic acetates **11**–**14** were found to be bound within the capsule, however, the time-averaged ^{1}H NMR spectra of these complexes carried out at room temperature, with the upfield shifts of their methyl protons less than 0.2 ppm, suggests that their molecular lengths are too short to fit within the cavity of capsule **1·4BF$_4$**. The exchange processes of these shorter guests probably occur through the opened spaces among the side arms of the capsule, and the dimensions of the cavity permit these guests to move freely within the cavity.

The binding abilities of guests **8**–**10** were much higher than those of the other aromatic acetates. Guests **8** and **9** are especially distinctive in terms of their binding abilities. The structures obtained by molecular modelling suggest that guests **8**, **9**, and **10** can be accommodated in the cavity. The methyl groups are placed near the end of the cavity, with close contact to the aromatic side walls, thus creating CH–π interactions (Figure 6).[21] Accordingly, more acidic methyl groups create more effective CH–π interactions to the aromatic walls of the capsule (Table 1).

Flexible alkyl diacetates **15**–**17** were accommodated within capsule **1·4BF$_4$**. Their ^{1}H NMR signals broadened in the presence of the capsule at room temperature; however, the protons of the encapsulated guests appeared as sharp signals at 218 K (Figure 7). At 218 K, the association constants of the guests with the capsule were determined. Surprisingly, the binding ability of **16** is about 150 times higher than those of **15** and **17**. This remarkably strict molecular recognition of the capsule is obviously based on the rigid and closed binding environment provided by the self-assembled capsule.

The signals of methyl groups of **15**–**17** were shifted higher than 0.0 ppm ($\Delta\delta = 3.5$ ppm), indicating that the methyl groups are situated near the ends of the capsule, as found

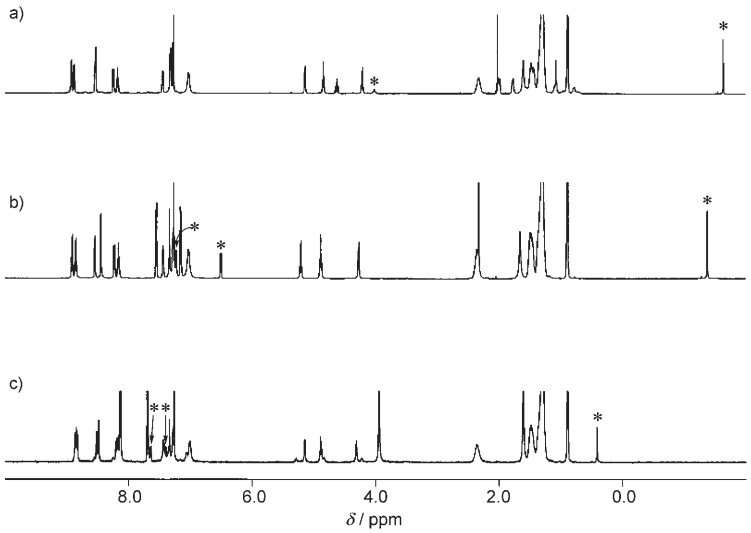

Figure 5. ^{1}H NMR of the supramolecular complexes of capsule **1·4BF$_4$** with a) **8**, b) **9**, c) **10** in $CDCl_3$ at 298 K. The bound guests are marked with *.

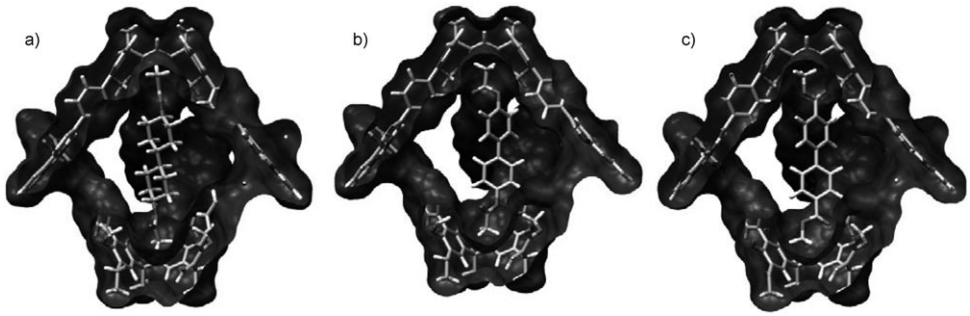

Figure 6. Computer-generated structures of the host–guest complexes of **1·4BF$_4$** with a) **8**, b) **9**, or c) **10**.

Table 1. Association constants (K_a) and free energy (ΔG) of guests **8**–**14** with the capsule in [D_1]chloroform at 298 K.

Guest	K_a [M^{-1}]	$-\Delta G$ [kcal mol^{-1}]
8	170000 ± 20000	7.13
9	82000 ± 2000	6.70
10	410 ± 10	3.56
11	118 ± 5	2.82
12	80 ± 10	2.59
13	60 ± 8	2.42
14	113 ± 6	2.80
15	33 ± 1[a]	1.51[a]
16	4900 ± 500[a]	3.68[a]
17	73 ± 1[a]	1.86[a]

[a] Association constants were determined at 218 K in [D_1]chloroform.

for guests **8**–**10**, even though guests **15**–**17** are conformationally more flexible than the others. The methylene protons adjacent to the acetoxyl group commonly display a sharp triplet resonance due to unrestricted rotation around the single bonds; however, they are already magnetically nonequivalent in the bound states in all cases due to the chiral nature of the capsule.

Molecular modelling clearly shows that diacetates **15** and **16** can be encapsulated in the cavity in their fully extended conformation, but **17** is too long to be incorporated in its extended form: their calculated molecular lengths are 14.5, 15.8, and 17.0 Å for **16**, **17**, and **18**, respectively. Yet, all of them are encapsulated as shown by the ^{1}H NMR spectra. The calculated structures of their complexes with the capsule gave insight into their binding conformations (Figure 8). Molecular modelling confirmed that diacetates **15** and **16** are lying in an elongated manner within the cavity, with the methyl groups positioned close to the ends. This is consistent with the ^{1}H NMR spectra of the complexes.

Coiling into a helix is one of the ways for an alkyl chain to decrease its length in a restricted space. Rebek and co-workers have recently reported that long alkyl chains show helical folding within cylindrical capsules.[22] The calculated structure of bound diacetate **17** suggests that it can adopt a helical conformation to fit within the cavity. The signals for the methylene group next to the acetoxyl group of diacetate **17** were well split and of AB type, which supports the suggestion that **17** adopted a helical conformation within the cavity (Figure 8c).

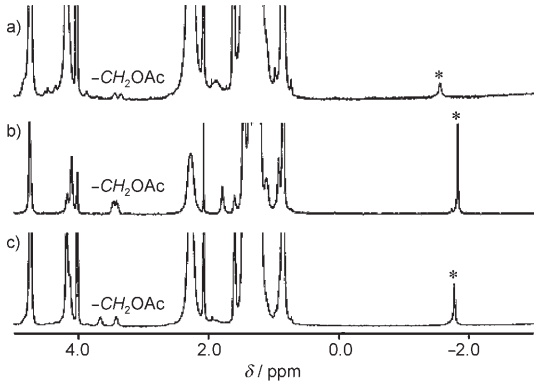

Figure 7. ^{1}H NMR spectra of the host–guest complexes of **1·4BF$_4$** with a) **15**, b) **16**, or c) **17** in [D_1]chloroform at 218 K. The methyl protons of the bound guests are marked with *.

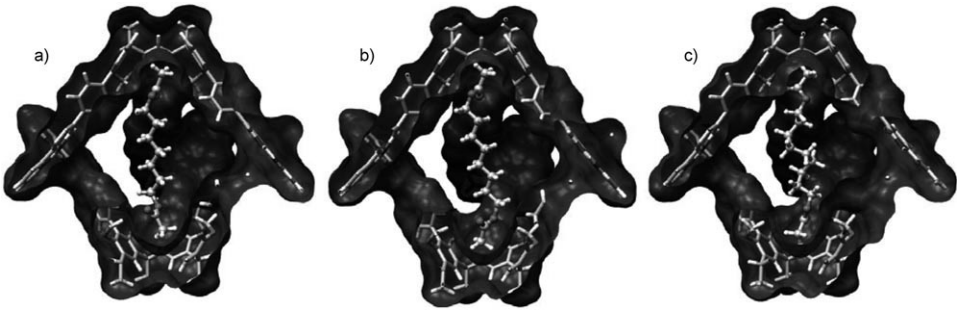

Figure 8. The calculated structures of the complexes of **1·4BF$_4$** with a) **15**, b) **16**, or c) **17**.

Thermodynamic studies of the complexation: Van't Hoff analysis of the guest encapsulations provides further insights into the role of the huge cavity of capsule **1·4BF$_4$** (Figure 9).

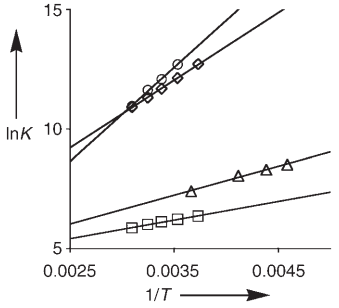

Figure 9. Van't Hoff plots for guests **8** (○), **9** (◇), **10** (□), and **16** (△).

The association constants of guests **8**, **9**, **10**, and **16** were determined at four different temperatures for each guest. The plots gave good linear correlations and so provided thermodynamic parameters for their encapsulation (Table 2). Comparison of the relative enthalpic and entropic components of the four complexes of **1·4BF$_4$** with **8**, **9**, **10**, or **16** provides a more detailed picture of the driving forces for their encapsulation. The enthalpic component of the stabilities of the complexes is undoubtedly composed of a variety of noncovalent interactions: van der Waals, electrostatic, CH–π, and others.

Table 2. Thermodynamic parameters for the encapsulation of guests **8**, **9**, **10**, and **16** in [D$_1$]chloroform.

Guest	ΔH [kcal mol^{-1}]	ΔS [cal mol^{-1} K^{-1}]
8	−7.8 ± 0.2	−2.4 ± 0.8
9	−5.61 ± 0.06	4.2 ± 0.2
10	−1.55 ± 0.08	6.8 ± 0.5
16	−2.4 ± 0.1	5.9 ± 0.6

Encapsulation of guests **8**, **9**, and **10** are enthalpically favored, most likely because of their size and shape. The large enthalpic difference ($\Delta\Delta H = 4.06$ kcal mol^{-1}) for encapsulation between **9** and **10** most likely comes from CH–π interactions of the more acidic methyl protons of **9**.

Complexes of **1·4BF$_4$** with **9**, **10**, or **16** have large favorable entropic components. As associations of two or more molecular components are commonly entropically unfavorable, the trends for **1·4BF$_4$** are unexpected. One plausible explanation can be given in terms of the desolvation of the cavity.[23] The self-assembled capsule **1·4BF$_4$** has an extremely large cavity whose interior can be occupied by several chloroform molecules. Encapsulation of the guests within the cavity forces the solvents out of the cavity. The positive entropic changes of the guest encapsulations are rationalized in terms of the desolvation of the solvated interior of the cavity.

The compensation relationship[24] between the enthalpic and entropic changes was observed here with the supramolecular complexations (Table 2). It shows that the stronger the attractive interaction between the host and guest, the more reduced the freedom of the guest movement in the supramolecular complex, which results in an entropic loss. Indeed, **8** receives the largest enthalpic gain during the complexation, but has to pay the largest entropic cost, the contribution of which is larger than that of the desolvation. The enthalpic gain of **16** with complexation is the smallest, which suggests that the guest still has some freedom of movement in the cavity, which is of course smaller than the available space on the outside of the cavity. In this case, the contribution of the desolvation overcomes the entropic loss due to the restriction of the freedom of the guest's movement in the complex. Accordingly, both the solvation–desolvation and change of the freedom of the guest's movement play an important role in the complex formation in organic media.

Co-encapsulation of carboxylic acids: Rebek and co-workers have shown that a cylindrical capsule encapsulated benzoic acids and pyridone as hydrogen-bonded homodimeric forms.[25] The different carboxylic acids form statistical mixtures of the homo and the hetero hydrogen-bonded dimers in organic solution. If one of them is complementary to the interior of the capsule, the capsule enhances this dimerization within the cavity (Scheme 3).

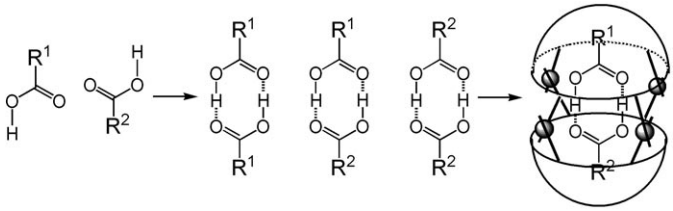

Scheme 3. Schematic representation of the selective encapsulation of the hydrogen-bonded heterodimer.

The molecular lengths of the dimers formed among carboxylic acids **18**, **19**, and **20** were calculated by using molecular mechanics calculations (Table 3). Molecular modelling

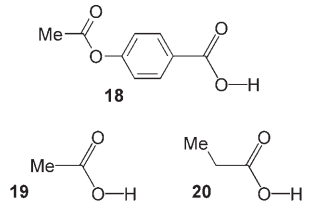

Table 3. Calculated molecular lengths of the hydrogen-bonded dimers formed by the combination of carboxylic acids **18**, **19**, and **20**.

Dimer	Molecular length [Å]
19·19	6.84
19·20	7.54
20·20	8.46
18·19	13.19
18·20	13.92
18·18	19.59

suggested that only heterodimers **18·19** and **18·20** have molecular lengths complementary to the cavity; those of the other dimers differ from the complementary length by about 14 Å.

When a 1:1 mixture of **18** and **19** was added to the solution of **1·4BF$_4$**, an asymmetrically filled capsule was exclusively observed at 218 K (Figure 10a). Two singlets appeared

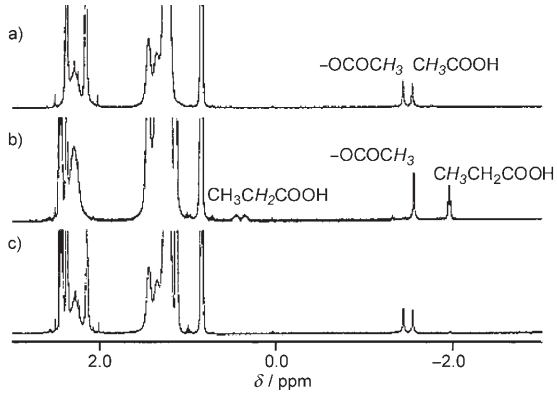

Figure 10. ^{1}H NMR spectra of the host–guest complexes of **1·4BF$_4$** with a) a 1:1 mixture of **18** and **19**, b) a 1:1 mixture of **18** and **20**, and c) a 1:1:1 mixture of **18**, **19**, and **20** in [D$_1$]chloroform at 218 K.

in the clear window higher than $\delta = 0$ ppm, assigned to the methyl groups of **18** and **19** ($\delta = -1.43$ ppm, $\Delta\delta = -3.8$ ppm for **18**; $\delta = -1.54$ ppm, $\Delta\delta = -3.7$ ppm for **19**) by a 2D-EXSY experiment. These characteristic upfield shifts of the methyl groups and the integrations confirmed the formation of the hydrogen-bonded heterodimer **18·19** in the capsule. Propionic acid **20** also forms a hydrogen-bonded heterodimer with **18** in the capsule. The characteristic upfield shifts were observed for the $-CH_3$ and $-CH_2-$ of **20** ($\Delta\delta = -3.1$ and -2.0 ppm for $-CH_3$ and $-CH_2-$, respectively), placing both $-CH_3$ groups near the ends of the cavity (Figure 10b).

The relative stability of the heterodimers was studied by a competition experiment. When **18**, **19**, and **20** were added in a 1:1:1 ratio into a solution of **1·4BF$_4$** in chloroform, the heterodimer **18·19** formed exclusively. The molecular modelling of the complexes provided plausible structures of the dimers within the cavity. Figure 11 shows that both hetero-

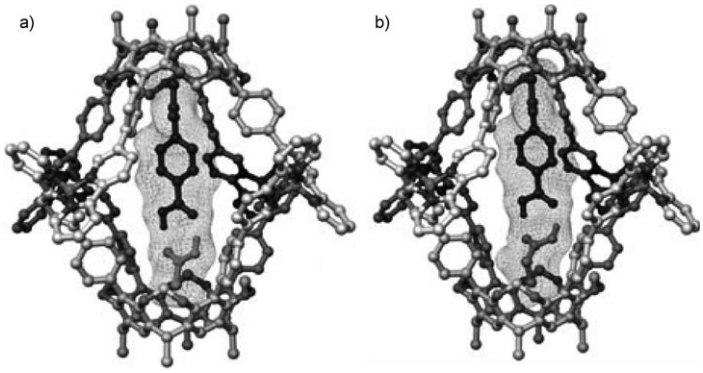

Figure 11. Calculated structures of the host–guest complexes of **1·4BF$_4$** with a) **18·19** or b) **18·20**.

dimers fit well inside the cavity, and that the methyl groups of **18**, **19**, and **20** point down to the ends of the cavity, creating CH–π interactions. The more acidic methyl group of **19** shows a more attractive CH–π interaction with the aromatic cavity. Accordingly, the CH–π interaction between the methyl groups and the aromatic interior of the cavity could account for the highly selective encapsulation of dimer **18·19**.

Capsule **1·4BF$_4$** is D_4 symmetric, meaning that the capsule exists as a racemic mixture, *P* and *M* forms, which equilibrates slowly on an NMR timescale. When a chiral guest is encapsulated, the guest-encapsulated capsule is diastereomeric, and the population of the two diastereomers can be determined by using spectroscopic methods.[26] 4,4′-Diacetoxybiphenyl **9** is shown to be a good guest. When capsule **1·4BF$_4$** was added to the solution of racemic **21**, the *para*-acetylmethyl groups appeared higher than $\delta = 0$ ppm with two sharp signals of unequal intensities, which indicates that the chiral capsule gives a diastereomeric selection of 26% (Figure 12).

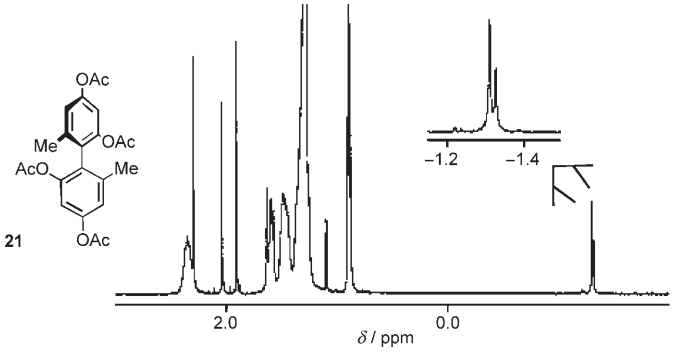

Figure 12. ^{1}H NMR spectrum of the complex of **1·4BF$_4$** with **21**. The inset shows the enlargement of the upfield signals.

Conclusion

We have presented the synthesis and encapsulation properties of the metal-coordination-driven self-assembling capsule **1·4BF$_4$** based on cavitand **2**. The capsule is an excellent model for studying the noncovalent interactions for guest selection as well as the desolvation of the interior of the large cavity. Encapsulation of the guests, as individual and as pairs, is unique to the capsule; in particular, pair-wise encapsulation of two different guests suggests the possibility that the capsule acts as a supramolecular catalyst. Diastereomeric-selective encapsulation of the capsule is just one of the interesting properties displayed. We will report on these properties in due course.

Experimental Section

General: ^{1}H NMR spectra were measured with a JEOL ECA 600, a JEOL Lambda 500, or a Varian Mercury 300 spectrometer using a residual solvent signal as internal standard. ^{13}C NMR spectra were taken with a JEOL Lambda 500 or a Varian Mercury 300 spectrometer. ^{13}C NMR chemical shifts (δ) were with reference to internal [D$_1$]chloroform (δ = 77.0 ppm) and carbon disulfide (δ = 192.8 ppm). All NMR spectra were recorded in $CDCl_3$ unless otherwise indicated. IR spectra were measured on a JASCO FT/IR-420S spectrometer. Mass spectra were recorded with a JEOL JMX-SX 102 mass spectrometer. Elemental analyses were performed on a Perkin Elmer 2400CHN elemental analyzer. Melting points were measured with a Yanagimoto micro melting point apparatus and are uncorrected. UV spectra were measured on a JASCO V-560 spectrometer.

All reactions were carried out under an argon atmosphere unless otherwise noted. THF, Et_2O, toluene, and dioxane were freshly distilled from sodium benzophenone. Dichloromethane and pyridine were freshly distilled from CaH_2. MeOH and EtOH were freshly distilled from activated magnesium. Column chromatography was performed using Merck silica gel (70–230 mesh).

Molecular mechanics calculations were performed with the MacroModel V6.5 program package running on a SGI O2. A low-mode search option was used for the initial geometry generation, and the given geometries were optimized by a conjugate gradient energy minimization using the amber* force field.

Determination of the association constants for guests **8**–**17** was carried out by means of a ^{1}H NMR titration technique in [D$_1$]chloroform. The complexes of **8**–**10** and **15**–**17** with **1·4BF$_4$** were in slow exchange on the NMR timescale and displayed well-resolved signals for the free and bound guests. In these cases the relative intensity of the protons of the free and bound guests, along with the known concentrations of the guests and **1·4BF$_4$**, were used to determine the association constants. In contrast, the complexes of the other guests with **1·4BF$_4$** were in fast exchange on the NMR timescale and showed only one set of resonances for the guest protons. In these cases, the association constants were determined by nonlinear-curve fitting analysis of the complexation-induced upfield-shifted data of the methyl protons upon the addition of **1·4BF$_4$**.

Thermodynamic parameters were determined by van't Hoff analyses using the association constants determined at different temperatures. **8**: $K_a = 57000 \pm 2000$ (323 K), 111000 ± 7000 (308 K), 170000 ± 20000 (296 K), 320000 ± 10000 M^{-1} (283 K); **9**: $K_a = 54000 \pm 5000$ (323 K), 82000 ± 7000 (308 K), 110000 ± 10000 (296 K), 183000 ± 8000 (283 K), 320000 ± 40000 M^{-1} (268 K); **10**: $K_a = 340 \pm 10$ (323 K), 400 ± 10 (308 K), 450 ± 10 (296 K), 500 ± 20 (283 K), 570 ± 10 M^{-1} (268 K); **16**: $K_a = 1600 \pm 200$ (273 K), 3000 ± 200 (243 K), 4000 ± 600 (228 K), 4900 ± 500 M^{-1} (218 K).

The complexation-induced shifts (CIS) for the protons of the guests are listed. The CIS values of the methyl protons for guests **11**, **12**, and **13** were derived by means of nonlinear curve fitting analyses. **8**: $\Delta\delta$ −3.66 (COCH_3), −0.60 ppm (CHOAc); **9**: $\Delta\delta$ −3.70 (COCH_3), −0.67 (Ar−H_o), −0.32 ppm (Ar−H_m); **10**: $\Delta\delta$ −3.53 (OCH_3), −0.48 (Ar−H_o), −0.29 ppm (Ar−H_m); **11**: $\Delta\delta$ −0.03 ppm (COCH_3); **12**: $\Delta\delta$ −0.10 ppm (COCH_3); **13**: $\Delta\delta$ −0.08 ppm (COCH_3); **15**: $\Delta\delta$ −3.65 (COCH_3), −0.62 ppm (CH_2OAc); **16**: $\Delta\delta$ −3.92 (COCH_3), −0.58 ppm (CH_2OAc); **17**: $\Delta\delta$ −3.86 (COCH_3), −0.47 ppm (CH_2OAc).

5-(4-Pinacolborylphenyl)-2,2′-bipyridine (5): [Pd(PPh$_3$)$_4$] (15 mol %) and Na_2CO_3 (2 M, 67 mL) were added to a solution of 5-bromobipyridine **3** (6.1 g, 26 mmol) and **4** (22 g, 66 mmol) in dioxane (100 mL) and ethanol (67 mL). After stirring for 4 h at 80 °C in the dark, the reaction mixture was poured into aqueous NH_4Cl and extracted with chloroform. The organic layer was dried over Na_2SO_4 and concentrated in vacuo. The residue was purified by column chromatography on silica gel to give the desired compound **5** (4.6 g, 49 %). M.p. 167–169 °C; ^{1}H NMR (300 MHz, $CDCl_3$): δ = 8.93 (d, J = 2.4 Hz, 1H), 8.70 (d, J = 5.1 Hz, 1H), 8.47 (d, J = 8.2 Hz, 1H), 8.44 (d, J = 7.6 Hz, 1H), 8.04 (dd, J = 8.2, 2.4 Hz, 1H), 7.93 (d, J = 8.2 Hz, 2H), 7.83 (dt, J = 7.6, 1.6 Hz, 1H), 7.66 (d, J = 8.2 Hz, 2H), 7.32 (ddd, J = 7.6, 5.1, 1.1 Hz, 1H), 1.37 ppm (s, 12H); ^{13}C NMR (75 MHz, $CDCl_3$): δ = 155.8, 155.1, 149.2, 147.7, 140.2, 136.9, 136.2, 135.5, 135.2, 126.3, 123.7, 121.0, 120.9, 83.9, 24.8 ppm; elemental analysis calcd (%) for $C_{22}H_{23}BN_2O_2$: C 73.76, H 6.47, N 7.82; found: C 73.66, H 6.43, N 7.99.

Tetraiodo cavitand 7: A butyllithium solution (1.8 mL of a 1.59 M solution) was slowly added to a solution of cavitand **6** (1.0 g 0.70 mmol) in anhydrous THF (56 mL) at −78 °C under an argon atmosphere. The reaction mixture was stirred for 1 h, and I_2 (2.0 g, 7.8 mmol) in THF (5 mL) was added at −78 °C. The reaction mixture was poured into aqueous NH_4Cl and extracted with ethyl acetate. The organic layer was washed with aqueous $Na_2S_2O_3$ and aqueous $NaHCO_3$, and dried over Na_2SO_4. The organic layer was concentrated in vacuo. The residue was purified by column chromatography on silica gel to give desired cavitand **7** (921 mg, 79 %). M.p. 112–113 °C; ^{1}H NMR (300 MHz, $CDCl_3$): δ = 7.05 (s, 4H), 5.96 (d, J = 7.4 Hz, 4H), 4.84 (t, J = 8.2 Hz, 4H), 4.31 (d, J = 7.4 Hz, 4H), 2.15–2.22 (m, 8H), 1.26–1.39 (m, 72H), 0.88 ppm (t, J = 6.3 Hz, 12H); ^{13}C NMR (75 MHz, $CDCl_3$): δ = 154.8, 138.7, 120.6, 98.7, 93.0, 37.9, 31.9, 30.0, 29.6, 29.3, 27.7, 22.6, 14.1; elemental analysis calcd (%) for $C_{76}H_{108}O_8I_4 \cdot {}^1/_2C_6H_{14}$: C 55.80, H 6.82; found: C 55.54, H 7.04.

Octadentate cavitand 2: H_2O (12 mL), bipyridine **5** (5.0 g, 14 mmol), and $AsPh_3$ (1.7 g, 5.5 mmol) in dioxane (200 mL) were added to a mixture of **7** (2.3 g, 1.4 mmol), [PdCl$_2$(PPh$_3$)$_2$] (500 mg, 50 mol %), and Cs_2CO_3 (14 g, 42 mmol) in dioxane (300 mL). After stirring for 5 h at 120 °C in the dark, the reaction mixture was filtered on a celite pad and the solution was concentrated in vacuo. The residue was purified by GPC and column chromatography on Al_2O_3 to give **2** (2.3 g, 80 %). M.p. 295 °C; ^{1}H NMR (500 MHz, $CDCl_3$) δ = 8.91 (d, J = 2.4 Hz, 4H), 8.66 (d, J = 4.9 Hz, 4H), 8.44 (d, J = 8.2 Hz, 4H), 8.41 (d, J = 7.9 Hz, 4H), 8.01 (dd, J = 8.2, 2.4 Hz, 4H), 7.81 (dt, J = 7.9, 1.8 Hz, 4H), 7.64 (d, J = 8.2 Hz, 8H), 7.39 (s, 4H), 7.29 (dd, J = 7.9, 4.9 Hz, 4H), 7.22 (d, J = 8.2 Hz, 8H), 5.41 (d, J = 7.0 Hz, 4H), 4.92 (t, J = 8.2 Hz, 4H), 4.39 (d, J = 7.0 Hz, 4H), 2.37–2.41 (m, 8H), 1.29–1.52 (m, 72H), 0.89 ppm (t, J = 6.7 Hz, 12H); ^{13}C NMR (75 MHz, $CDCl_3$): δ = 155.8, 155.0, 152.7, 149.2, 147.5, 138.5, 136.9, 136.3, 135.7, 135.0, 133.9, 130.7, 128.7, 126.5, 123.6, 121.0, 120.9, 120.1, 100.6, 37.1, 31.9, 30.5, 29.8, 29.7, 29.4, 28.0, 22.7, 14.1 ppm; elemental analysis calcd (%) for $C_{140}H_{152}N_8O_8$: C 81.05, H 7.38, N 5.40; found: C 80.81, H 7.35, N 5.32.

Self-assembled capsule 1·4BF$_4$: $AgBF_4$ (83.0 mg, 0.43 mmol) in nitromethane (5 mL) was added to a solution of **2** (440 mg, 0.21 mmol) in chloroform (20 mL). The reaction mixture was stirred for several hours and the solvent was removed in vacuo. The crude compound was recrystallized from chloroform and hexane (7:3) to give desired compound **1·4BF$_4$** (498 mg, 95 %). M.p. >300 °C; ^{1}H NMR (500 MHz, $CDCl_3$): δ = 8.88 (d, J = 8.5 Hz, 8H), 8.85 (d, J = 7.9 Hz, 8H), 8.55 (d, J = 5.2 Hz, 8H), 8.49 (s, 8H), 8.26 (dd, J = 8.5, 2.0 Hz, 8H), 8.17 (t, J = 7.9 Hz, 8H), 7.45 (dd, J = 7.9, 5.2 Hz, 8H), 7.36 (d, J = 8.2 Hz, 16H), 7.29 (s, 8H), 7.06 (d, J = 8.2 Hz, 16H), 5.28 (d, J = 6.7 Hz, 8H), 4.82 (t, J = 7.9 Hz, 8H), 4.21 (d,

J=6.7 Hz, 8H), 2.28–2.34 (m, 16H), 1.27–1.47 (m, 144H), 0.88 ppm (t, J=6.7 Hz, 24H); ^{13}C NMR (75 MHz, $CDCl_3$): δ=152.6, 152.3, 151.9, 150.4, 150.3, 148.7, 139.7, 138.6, 138.3, 137.9, 135.5, 133.8, 131.0, 128.0, 126.7, 125.3, 124.2, 120.1, 100.6, 37.1, 31.9, 30.5, 29.8, 29.7, 29.4, 27.9, 22.7, 14.1 ppm; elemental analysis calcd (%) for $C_{280}H_{304}Ag_4B_4F_{16}N_{16}O_{16}$: C 68.24, H 6.22, N 4.55; found: C 68.00, H 6.31, N 4.49.

[1] For reviews on large cavities, see: a) D. M. Rudkevich, J. Rebek, Jr., *Eur. J. Org. Chem.* **1999**, 1991–2005; b) D. M. Rudkevich, *Chem. Eur. J.* **2000**, *6*, 2679–2689; c) D. J. Cram, *Science* **1983**, *219*, 1177–1183; d) C. D. Gutsche, *Calixarenes Revisited*, The Royal Society of Chemistry, Cambridge, **1998**; e) D. M. Rudkevich in *Functional Synthetic Receptors* (Eds.: T. Schrader, A. D. Hamilton), Wiley, Weinheim, **2005**, pp. 257–298.

[2] For reviews on carceplexes and hemicarceplexes, see: a) E. Maverick, D. J. Cram, *Compr. Supramol. Chem.* **1996**, *2*, 367–418; b) D. J. Cram, *Nature* **1992**, *356*, 29–36; c) J. C. Sherman, *Tetrahedron* **1995**, *51*, 3395–3422; d) R. G. Chapman, J. C. Sherman, *Tetrahedron* **1997**, *53*, 15911–15945; e) A. Jasat, J. C. Sherman, *Chem. Rev.* **1999**, *99*, 931–967; f) H.-J. Choi, D. J. Cram, C. B. Knobler, E. F. Marverick, *Pure Appl. Chem.* **1993**, *65*, 539–543.

[3] For reviews on self-assembling capsules and cages, see: a) J. Rebek, Jr., *Angew. Chem.* **2005**, *11*, 2104–2115; *Angew. Chem. Int. Ed.* **2005**, *44*, 2068–2078; b) J. Rebek, Jr., *Chem. Soc. Rev.* **1996**, 255–264; c) M. M. Conn, J. Rebek, Jr., *Chem. Rev.* **1997**, *97*, 1647–1668; d) F. Hof, J. Rebek, Jr., *Proc. Natl. Acad. Sci. USA* **2002**, *99*, 4775–4777; e) F. Hof, S. L. Craig, C. Nuckolls, J. Rebek, Jr., *Angew. Chem.* **2002**, *114*, 1556–1578; *Angew. Chem. Int. Ed.* **2002**, *41*, 1488–1508; f) L. J. Prins, D. N. Reinhoudt, P. Timmerman, *Angew. Chem.* **2001**, *113*, 2446–2492; *Angew. Chem. Int. Ed.* **2001**, *40*, 2382–2426.

[4] a) T. Heinz, D. M. Rudkevich, J. Rebek, Jr., *Nature* **1999**, *37*, 3410–3413; b) F. C. Tucci, D. M. Rudkevich, J. Rebek, Jr., *J. Am. Chem. Soc.* **1999**, *121*, 4928–4929; c) R. S. Meissner, J. Rebek, Jr., J. D. Mendoza, *Science* **1995**, *270*, 1485–1488; d) K. D. Shimizu, J. Rebek, Jr., *Proc. Natl. Acad. Sci. USA* **1995**, *92*, 12403–12407; e) B. C. Hamann, K. D. Shimizu, J. Rebek, Jr., *Angew. Chem.* **1996**, *108*, 1425–1427; *Angew. Chem. Int. Ed. Engl.* **1996**, *35*, 1326–1329; f) R. K. Castellano, D. M. Rudkevich, J. Rebek, Jr., *J. Am. Chem. Soc.* **1996**, *118*, 10002–10003; g) N. Branda, R. M. Grotzfeld, C. Valdés, J. Rebek, Jr., *J. Am. Chem. Soc.* **1995**, *117*, 85–88; h) B. M. O'Leary, R. M. Grotzfeld, J. Rebek, Jr., *J. Am. Chem. Soc.* **1997**, *119*, 11701–11702; i) J. M. Rivera, T. Martín, J. Rebek, Jr., *J. Am. Chem. Soc.* **1998**, *120*, 819–820; j) B. M. O'Leary, T. Szabo, N. Svenstrup, C. A. Schalley, A. Lützen, M. Schäfer, J. Rebek, Jr., *J. Am. Chem. Soc.* **2001**, *123*, 11519–11533; k) D. W. Johnson, F. Hof, P. M. Iovine, C. Nuckolls, J. Rebek, Jr., *Angew. Chem.* **2002**, *114*, 3947–3950; *Angew. Chem. Int. Ed.* **2002**, *41*, 3793–3796; l) L. R. MacGillivray, J. L. Atwood, *Nature* **1997**, *389*, 469–472; m) A. Shivanyuk, J. Rebek, Jr., *Proc. Natl. Acad. Sci. USA* **2001**, *98*, 7662–7665; n) R. E. Brewster, S. B. Shuker, *J. Am. Chem. Soc.* **2002**, *124*, 7902–7903; o) L. R. MacGillivray, P. R. Diamente, J. L. Reid, J. A. Ripmeester, *Chem. Commun.* **2000**, 359–360; p) C. M. Drain, R. Fischer, E. G. Nolen, J.-M. Lehn, *J. Chem. Soc. Chem. Commun.* **1993**, 243–245; q) K. Kobayashi, T. Shirasaka, K. Yamaguchi, S. Sakamoto, E. Horn, N. Furukawa, *Chem. Commun.* **2000**, 41–42; r) K. Kobayashi, K. Ishii, S. Sakamoto, T. Shirasaka, K. Yamaguchi, *J. Am. Chem. Soc.* **2003**, *125*, 10615–10624.

[5] a) S. R. Seidel, P. J. Stang, *Acc. Chem. Res.* **2002**, *35*, 972–983; b) Y. K. Kryschenko, S. R. Seidel, D. C. Muddiman, A. I. Nepomuceno, P. J. Stang, *J. Am. Chem. Soc.* **2003**, *125*, 9647–9652; c) K.-W. Chi, C. Addicott, Y. K. Kryschenko, P. J. Stang, *J. Org. Chem.* **2004**, *69*, 964–966; d) P. S. Mukherjee, N. Das, P. J. Stang, *J. Org. Chem.* **2004**, *69*, 3526–3529; e) D. L. Caulder, C. Brückner, R. E. Powers, S. König, T. N. Parac, J. A. Leary, K. E. Raymond, *J. Am. Chem. Soc.* **2001**, *123*, 8923–8938; f) M. Scherer, D. L. Caulder, D. W. Johnson, K. E. Raymond, *Angew. Chem.* **1999**, *111*, 1689–1694; *Angew. Chem. Int. Ed.* **1999**, *38*, 1588–1592; g) D. L. Caulder, R. E. Powers, T. N. Parac, K. E. Raymond, *Angew. Chem.* **1998**, *110*, 1940–1943; *Angew. Chem. Int. Ed.* **1998**, *37*, 1840–1843; h) T. N. Parac, D. L. Caulder, K. E. Raymond, *J. Am. Chem. Soc.* **1998**, *120*, 8003–8004; i) D. W. Johnson, J. Xu, R. W. Saalfrank, K. E. Raymond, *Angew. Chem.* **1999**, *111*, 3058–3061; *Angew. Chem. Int. Ed.* **1999**, *38*, 2882–2885; j) D. L. Caulder, K. E. Raymond, *J. Chem. Soc. Dalton Trans.* **1999**, 1185–1200; k) D. K. Chand, K. Biradha, M. Fujita, *Chem. Commun.* **2001**, 1652–1653; l) N. Takeda, K. Umemoto, K. Yamaguchi, M. Fujita, *Nature* **1999**, *398*, 794–796; m) T. Kusukawa, M. Fujita, *Angew. Chem.* **1998**, *110*, 3327–3329; *Angew. Chem. Int. Ed.* **1998**, *37*, 3142–3144; n) T. Kusukawa, M. Fujita, *J. Am. Chem. Soc.* **1999**, *121*, 1397–1398; o) M. Fujita, D. Oguro, M. Miyazawa, H. Oka, K. Yamaguchi, K. Ogura, *Nature* **1995**, *378*, 469–471; p) P. Baxter, J.-M. Lehn, A. DeCian, J. Fisher, *Angew. Chem.* **1993**, *105*, 92–95; *Angew. Chem. Int. Ed. Engl.* **1993**, *32*, 69; q) E. Leiz, A. V. Dorsselaer, R. Krämer, J.-M. Lehn, *J. Chem. Soc. Chem. Commun.* **1993**, 990; r) H. Sleiman, P. N. W. Baxter, J.-M. Lehn, K. Rissanen, *J. Chem. Soc. Chem. Commun.* **1995**, 715–716; s) G. S. Hanan, C. R. Arana, J.-M. Lehn, D. Fenske, *Angew. Chem.* **1995**, *107*, 1191; *Angew. Chem. Int. Ed. Engl.* **1995**, *34*, 1122–1124; t) A. Ikeda, Y. Yoshimura, H. Udzu, C. Fukuhara, S. Shinkai, *J. Am. Chem. Soc.* **1999**, *121*, 4296–4297.

[6] a) P. Jacopozzi, E. Dalcanale, *Angew. Chem.* **1997**, *109*, 665–667; *Angew. Chem. Int. Ed. Engl.* **1997**, *36*, 613–615; b) B. Bibal, B. Tinant, J.-P. Declercq, J.-P. Dutasta, *Chem. Commun.* **2002**, 432–433; c) S. J. Park, J.-I. Hong, *Chem. Commun.* **2001**, 1554–1555; d) K. Kobayashi, Y. Yamada, M. Yamanaka, Y. Sei, K. Yamaguchi, *J. Am. Chem. Soc.* **2004**, *126*, 13896–13897; e) O. D. Fox, J. F.-Y. Leung, J. M. Hunter, N. K. Dalley, R. G. Harrison, *Inorg. Chem.* **2000**, *39*, 783–790; f) O. D. Fox, E. J. S. Wilkinson, P. D. Beer, M. G. B. Drew, *Chem. Commun.* **2000**, 391–392.

[7] T. Haino, M. Kobayashi, M. Chikaraishi, Y. Fukazawa, *Chem. Commun.* **2005**, 2321–2323.

[8] F. Mohamadi, N. G. J. Richards, W. C. Guida, R. Liskamp, M. Lipton, C. Caufield, G. Chang, T. Hendrickson, W. C. Still, *J. Comput. Chem.* **1990**, *11*, 440–467.

[9] A. Nicholls, K. A. Sharp, B. Honig, *Proteins* **1991**, *11*, 281.

[10] F. M. Romero, R. Ziessel, *Tetrahedron Lett.* **1995**, *36*, 6471–6474.

[11] M. H. Todd, S. Balasubramanian, C. Abell, *Tetrahedron Lett.* **1997**, *38*, 6781–6784.

[12] P. Timmerman, H. Boerrigter, W. Verboom, G. J. Van Hummel, S. Harkema, D. N. Reinhoudt, *J. Inclusion Phenom. Mol. Recognit. Chem.* **1994**, *19*, 167–191.

[13] L. Sebo, F. Diederich, V. Gramlich, *Helv. Chim. Acta* **2000**, *83*, 93–113.

[14] D. C. Teller, E. Swanson, C. DeHaen, *Methods in Enzymology Vol. 61*, Academic Press, New York, **1979**, pp. 103–124.

[15] Y. Cohen, L. Avram, L. Frish, *Angew. Chem.* **2005**, *117*, 524–560; *Angew. Chem. Int. Ed.* **2005**, *44*, 520–554.

[16] a) M. S. Kaucher, Y.-F. Lam, S. Pieraccini, G. Bottarelli, J. T. Davis, *Chem. Eur. J.* **2005**, *11*, 164–173; b) L. Avram, Y. Cohen, *Org. Lett.* **2003**, *5*, 1099–1102.

[17] E. O. Stejskal, J. E. Tanner, *J. Chem. Phys.* **1965**, *42*, 288–292.

[18] a) A. S. Altieri, D. P. Hinton, R. A. Byrd, *J. Am. Chem. Soc.* **1995**, *117*, 7566–7567; b) V. V. Krishnan, *J. Magn. Reson.* **1997**, *124*, 468–473.

[19] a) L. C. Palmer, J. Rebek, Jr., *Org. Biomol. Chem.* **2004**, *2*, 3051–3059; b) C. L. Perrin, T. J. Dwyer, *Chem. Rev.* **1990**, *90*, 935–967.

[20] T. Haino, H. Araki, Y. Yamanaka, Y. Fukazawa, *Tetrahedron Lett.* **2001**, *42*, 3203–3206.

[21] a) K. Kobayashi, Y. Asakawa, Y. Kikuchi, H. Toi, Y. Aoyama, *J. Am. Chem. Soc.* **1993**, *115*, 2648–2654; b) D. Falábu, A. Shivanyuk, M. Nissinen, K. Rissanen, *Org. Lett.* **2002**, *4*, 3019–3022.

[22] A. Scarso, L. Trembleau, J. Rebek, Jr., *J. Am. Chem. Soc.* **2004**, *126*, 13512–13518.

[23] a) J. Kang, J. Rebek, Jr., *Nature* **1996**, *382*, 239–241; b) R. M. Grotzfeld, N. Branda, J. Rebek, Jr., *Science* **1996**, *271*, 487–489.

[24] a) Y. Inoue, T. Hakushi, *J. Chem. Soc. Perkin Trans. 2* **1985**, 935–946; b) Y. Inoue, F. Amano, N. Okada, H. Inada, M. Ouchi, A. Tai, T. Hakushi, Y. Lu, L.-H. Tong, *J. Chem. Soc. Perkin Trans. 2* **1990**,

1239–1246; c) D. B. Smithrud, T. B. Wyman, F. Diederich, *J. Am. Chem. Soc.* **1991**, *113*, 5420–5426.

[25] Benzoic acids and methylpyridone formed homodimers in the self-assembled cylindrical capsule. See: T. Heinz, D. M. Rudkevich, J. Rebek, Jr., *Angew. Chem.* **1999**, *111*, 1206–1209; *Angew. Chem. Int. Ed.* **1999**, *38*, 1136–1139.

[26] a) J. M. Rivera, T. Martín, J. Rebek, Jr., *Science* **1998**, *279*, 1021–1023; b) J. M. Rivera, T. Martín, J. Rebek, Jr., *J. Am. Chem. Soc.* **2001**, *123*, 5213–5220; c) R. K. Castellano, B. H. Kim, J. Rebek, Jr., *J. Am. Chem. Soc.* **1997**, *119*, 12671–12672; d) R. K. Castellano, C. Nuckolls, J. Rebek, Jr., *J. Am. Chem. Soc.* **1999**, *121*, 11156–11163.

Received: August 11, 2005
Revised: October 12, 2005
Published online: February 15, 2006

